



Published in final edited form as:

Mol Cancer Ther. 2018 May ; 17(5): 1079–1089. doi:10.1158/1535-7163.MCT-17-0137.

EGF Receptor and mTORC1 are novel therapeutic targets in nonseminomatous germ cell tumors

Kenneth S. Chen^{1,6,*}, Nicholas J. Fustino^{1,6,*}&, Abhay A. Shukla^{1,2}, Emily K. Stroup¹, Albert Budhipramono¹, Christina Ateek¹, Sarai H. Stuart^{1,4}, Kiyoshi Yamaguchi^{3,7}, Payal Kapur⁴, A. Lindsay Frazier⁸, Lawrence Lum³, Leendert H.J. Looijenga⁹, Theodore W. Laetsch^{1,6}, Dinesh Rakheja^{1,4,#}, and James F. Amatruda^{1,2,5,6,#}

¹Department of Pediatrics, University of Texas Southwestern Medical Center, Dallas, TX 75390, USA ²Department of Molecular Biology, University of Texas Southwestern Medical Center, Dallas, TX 75390, USA ³Department of Cell Biology, University of Texas Southwestern Medical Center, Dallas, TX 75390, USA ⁴Department of Pathology, University of Texas Southwestern Medical Center, Dallas, TX 75390, USA ⁵Department of Internal Medicine, University of Texas Southwestern Medical Center, Dallas, TX 75390, USA ⁶Margaret Gill Center for Cancer and Blood Disorders, Children's Health, Dallas, TX 75390, USA ⁷Division of Clinical Genome Research, Institute of Medical Science, University of Tokyo, Tokyo, Japan ⁸Department of Pediatric Oncology, Children's Hospital Dana-Farber Cancer Care, Boston MA 02115, USA ⁹Department of Pathology, Erasmus MC - University Medical Center Rotterdam, Rotterdam, The Netherlands

Abstract

Germ cell tumors (GCTs) are malignant tumors that arise from pluripotent embryonic germ cells and occur in children and young adults. GCTs are treated with cisplatin-based regimens which, while overall effective, fail to cure all patients and cause significant adverse late effects. The seminoma and non-seminoma forms of GCT exhibit distinct differentiation states, clinical behavior and response to treatment, however the molecular mechanisms of GCT differentiation are not fully understood. We tested whether the activity of the mammalian target of rapamycin complex 1 (mTORC1) and mitogen-activated protein kinase (MAPK) pathways were differentially active in the two classes of GCT. Here we show that non-seminomatous germ cell tumors (NSGCTs, including embryonal carcinoma, yolk sac tumor and choriocarcinoma) from both children and adults display activation of the mTORC1 pathway, while seminomas do not. In seminomas, high levels of REDD1 may negatively regulate mTORC1 activity. In NSGCTs, on the other hand, EGF and FGF2 ligands can stimulate mTORC1 and MAPK signaling, and members of

[#]To whom correspondence should be addressed. Dinesh Rakheja, Department of Pathology, Children's Health Children's Medical Center, 1935 Medical District Drive, Dallas, TX 75235; Tel: +1-214-456-2022; Fax: +1-214-456-4713; dinesh.rakheja@utsouthwestern.edu, or James F. Amatruda, Department of Pediatrics, University of Texas Southwestern Medical Center, 5323 Harry Hines Blvd., Dallas, TX 75390; Tel: +1-214-648-3896; Fax: +1-214-645-5915; james.amatruda@utsouthwestern.edu.

*equal contribution.

¤t address: Blank Children's Hospital, Des Moines, IA 50309 USA

Conflict of interest disclosure: A. Lindsay Frazier serve on the Clinical Advisory Board for Decibel Therapeutics. Theodore W. Laetsch is a Consultant for Loxo Oncology, Novartis, and Eli Lilly, and receives research funding from Pfizer.

the EGF and FGF receptor families are more highly expressed. Lastly, proliferation of NSGCT cells *in vitro* and *in vivo* is significantly inhibited by combined treatment with the clinically available agents erlotinib and rapamycin, which target EGFR and mTORC1 signaling, respectively. These results provide an understanding of the signaling network that drives GCT growth and a rationale for therapeutic targeting of GCTs with agents that antagonize the EGFR and mTORC1 pathways.

Keywords

EGFR; mTOR; non-seminomas; germ cell tumors

INTRODUCTION

Germ cell tumors (GCTs) are malignant cancers of the testis, ovary, or extragonadal sites such as retroperitoneum, mediastinum, and brain. In childhood and adolescence, GCTs account for 15% of malignancies. They also occur in adulthood, where they are the most common cancer in Caucasian men aged 15–40 (1,2). GCTs are believed to originate from pluripotent embryonic germ cells, which may explain the occurrence of a wide range of histologic appearances, often within the same tumor (1). GCTs that retain features of potentially pluripotent, primitive germ cells are called seminomas in the testis, dysgerminomas in the ovary, or germinomas in extragonadal sites (collectively referred to as “seminomas” here). Among non-seminomatous GCTs (NSGCTs), embryonal carcinoma exhibits a stem cell-like phenotype, while other NSGCTs exhibit differentiation into somatic tissues (teratoma) or extraembryonic-like structures, such as yolk sac and placenta (yolk sac tumor [YST] and choriocarcinoma, respectively).

GCTs may also be categorized by age at presentation. So-called Type I GCTs, which occur in young children aged 0–5 years, exhibit limited histologic diversity, being comprised of YSTs, teratomas or mixtures of the two. The current World Health Organization (WHO) classification of testis tumors refers to these tumors as Germ Cell Neoplasia in situ (GCNIS)-unrelated tumors. Type II GCTs of adolescents and adults exhibit more diverse histologies, including seminomas, non-seminomas (embryonal carcinoma, YST, choriocarcinoma or teratoma) or mixtures of seminomas and non-seminomas (1). Within the testis they are referred to as GCNIS-related GCTs.

Clinically, NSGCTs are more chemoresistant and radioresistant than seminomas. Biologically, seminomas and NSGCTs exhibit divergent DNA methylation patterns (3–5), copy number aberrations (6), somatic mutations (7), and gene expression profiles (8). However, despite significant differences in their biological and clinical behavior, all malignant GCTs, regardless of histology or age at presentation, continue to be treated using the same platinum-based chemotherapy regimens. As a result, children and adults with any malignant GCT are exposed to toxic effects of bleomycin, etoposide and cisplatin, the standards developed for testicular GCTs. While cisplatin-based regimens have generally produce good outcomes, platinum resistance is seen in up to 15% of GCTs and is much more common among non-seminomas (9,10). These resistant tumors have dismal outcomes,

underlining the need for novel therapeutic strategies, especially for non-seminomatous GCTs (11).

In many other cancer types, targeted therapies have revolutionized treatment regimens with the promise of overcoming chemoresistance and producing fewer toxicities. Kinase signaling pathways remain among the most attractive therapeutic targets in cancer, but the importance of various signaling pathways in GCT development remains poorly understood. Some previous data suggest that seminomas and NSGCTs utilize different signaling pathways. For example, we have previously demonstrated that the bone morphogenetic protein (BMP) signaling pathway is preferentially active in non-seminomas compared to seminomas (12,13). Similarly, Fritsch and co-workers showed that the Wnt/ β -catenin pathway is more active in NSGCTs than in seminomas (14). However, neither of these pathways is targetable with clinically available agents, and it remains unclear what other cellular pathways may act to govern survival or differentiation in GCTs.

Genetic studies in adult GCTs implicate importance of the mitogen-activated protein kinase (MAPK) pathway. Recurrent genomic aberrations have shown *KRAS* activation by somatic mutation or amplification (15) and somatic activating mutations in the *KIT* tyrosine kinase receptor (16–22). These mutations typically occur in seminomas. Additionally, risk loci near *SPRY4*, a negative regulator of EGF- and FGF-dependent MAPK signaling, have been identified in genome-wide association studies of testicular GCT in both adults (23,24) and adolescents (25).

A second pathway, the mammalian target of rapamycin complex 1 (mTORC1) signaling pathway, is of particular interest in GCTs because it has been shown to control differentiation of germline stem cells during normal development (26). One study identified a potential GCT risk polymorphism near *PTEN* (27), and recently mutations in *PIK3CA* and *AKT* have been identified in cisplatin-resistant GCTs (22). The mTORC1 pathway is a central regulator of cell growth, proliferation, and differentiation (28), and can be activated in parallel to the MAPK pathway. Like the MAPK pathway, mTORC1 signaling has emerged as a promising therapeutic target in many adult and pediatric cancers, particularly in renal cell carcinoma (29,30). However, the activity of the MAPK and mTORC1 signaling pathways have not been demonstrated in GCT samples.

In this study, we use immunohistochemistry (IHC) on a cohort of seminomatous and nonseminomatous GCTs to demonstrate highly active MAPK and mTORC1 activity in all malignant NSGCT histologies, as compared to seminomas. We show that seminomas express high levels of REDD1, a suppressor of mTORC1 signaling. In contrast, YSTs express high levels of epidermal growth factor (EGF) and fibroblast growth factor (FGF) receptors, which signal through the MAPK and mTORC1 pathways. Finally, we show that the EGFR inhibitor erlotinib and the mTORC1 inhibitor rapamycin together inhibit NSGCT cell proliferation *in vitro*. These results establish EGFR and mTORC1 inhibition as a novel therapeutic strategy for non-seminomatous GCTs and are the first demonstration of *in vitro* efficacy of targeted therapy in GCT.

MATERIALS AND METHODS

Tumor samples

The study was approved by the Institutional Review Board of the University of Texas Southwestern Medical Center. For samples from the Erasmus Medical Center, Rotterdam, use of the samples was approved by an institutional review board and they were used according to the 'Code for Proper Secondary Use of Human Tissue in The Netherlands', developed by the Dutch Federation of Medical Scientific Societies (FMWV) (version 2002, updated 2011) (31). All patients gave consent for use of tissue for research, and all studies were carried out in accordance with International Ethical Guidelines for Biomedical Research Involving Human Subjects (CIOMS) guidelines. A tissue microarray (TMA) was constructed consisting of paraffin-embedded tissue from 14 yolk sac tumors (YSTs), 9 seminomas (seminomas), 3 normal testes, and 3 normal ovaries, using tissue blocks were obtained from Children's Medical Center of Dallas. Tissue microarrays containing a further set of 260 GCT of diverse histologies were prepared at the Erasmus Medical Center, Rotterdam (32). All hematoxylin-eosin stained sections of each case were reviewed by a pathologist and representative sections were selected.

Immunohistochemistry

IHC was performed on Ventana Benchmark (phospho-mTOR, phospho-S6, Cyclin D1, HIF1A), Ventana Discovery (GLUT1, PLZF, p-ERK1/2) or Dako Link 48 (REDD1) automated immunostainers (Ventana, Tucson, AZ, USA; Dako, Carpinteria, CA, USA) using standard immunoperoxidase techniques and hematoxylin counterstaining. The immunohistochemical staining was scored by both the intensity of staining (0 – no staining, 1 – mild staining, 2 – moderate staining, 3 – strong staining) and the percentage of positively staining cells (0 – no staining, 1 – <10% cells staining, 2 – 10–50% cells staining, 3 – >50% cells staining). For each tumor, the intensity score and the percentage positivity score were an average of the scores for each of two cores in the TMA. A combined immunohistochemical score, ranging from 0 to 9, was calculated as the product of the average intensity score and the average percentage positivity score. Two-tailed *t* tests were used to compare the combined immunohistochemical scores for each antibody between histological subtypes.

Quantitative RT-PCR

Total RNA was prepared from up to 50 mg of fresh frozen tumor tissue in TRIzol® (Invitrogen, Carlsbad, CA) as per manufacturer recommendations. To remove contaminant genomic DNA, DNase digestion was done using RNase-Free DNase Digestion Kit on RNeasy columns (Qiagen, Valencia, CA). cDNA was synthesized from 1 µg of RNA using RT² First Strand Kit (SABiosciences, Frederick, MD). qPCR was performed on an ABI 7500 Real-Time PCR System (Applied Biosystems, Carlsbad, CA) using RT² SYBR® Green qPCR Master Mix (SABiosciences, Frederick, MD) per manufacturer's protocol. Primers for ERBB and FGFR family members were designed and validated. Gene expression was normalized to endogenous β-actin (*ACTB*) and glyceraldehyde-3-phosphate dehydrogenase (*GAPDH*). Gene expression was calculated using the 2^{-Ct} method, and *p* values were calculated using the two-tailed t-test.

Cell lines and treatments

NCCIT and NTERA-2 cells were obtained in 2015 from the American Type Culture Collection (ATCC; Manassas, VA) and passaged in RPMI-1640 and DMEM, respectively, supplemented with 10% fetal bovine serum. All cell lines were validated by STR profiling upon receipt from ATCC (UT Southwestern Genotyping Core Facility). Early-passage aliquots were frozen and revalidated prior to performing growth curve and xenograft experiments. All cells were tested for Mycoplasma contamination prior to use, using the MycoAlert Mycoplasma Detection Kit (Lonza). For drug treatments, cells were seeded in 6- or 12-well plates, and 24 hours later, the media was replaced with media containing drug or carrier. Cell lysates were harvested after overnight exposure. For ligand treatments, recombinant protein was added to the media 20 minutes prior to harvesting. Ligands were added to the media at the following final concentrations: BMP2 (100 ng/ml), Wnt3a (100 ng/ml), EGF (40 ng/ml), IGF-II (20 ng/ml), and FGF2 (40 ng/ml).

Immunoblotting

Cells were collected in ice-cold radio-immunoprecipitation assay buffer supplemented with protease inhibitor and phosphatase inhibitor, incubated on ice for 15 minutes, sonicated, and clarified by centrifugation. Protein concentrations were determined by BCA assay. Samples were separated on SDS-PAGE, transferred to polyvinylidene fluoride membrane and blocked in 1% casein in PBS. All primary antibodies were diluted in 1% casein in PBS with 0.1% Tween 20 and detected using HRP-linked secondary antibodies. Chemiluminescence was captured by exposure to X-ray film. Details of antibody catalog numbers and working concentrations are listed in Supplementary Material.

Cell proliferation assay

1×10^5 cells/well were seeded in 6-well plates. The next day, cells were treated in triplicate with 10 nM rapamycin, 1 μ M erlotinib, or both, or an equivalent volume of DMSO, in medium for up to six days. Each day, cells from three wells per condition were counted and discarded. Cells were counted in trypan blue using a hemacytometer.

Cell viability assay

1,000 cells per well were seeded in 96-well black, clear-bottom plates. The next day, media was replaced with media containing various concentrations of drug or an equivalent volume of DMSO. After 72 hours of incubation, resazurin dye was added to each well to a final concentration of 30 mcg/ml. After 3 hours the plate was read on a fluorescent plate reader at excitation and emission wavelengths of 560/620 nm. Experiments were performed with 5 replicates at each dose. Values represent mean \pm SEM.

Xenografts

For each cell line, subcutaneous xenografts were established in 32 six-week-old NOD-*scid* IL2Rg^{null} mice. 1×10^7 cells, resuspended in serum-free medium diluted 1:1 with matrigel, were subcutaneously implanted. Eleven days after injection, when tumors were palpable in all 32 mice, medication administration was initiated. The mice were randomized into four groups of n=8 mice each: vehicle only; rapamycin only; erlotinib only; or both rapamycin

and erlotinib. Rapamycin (LC Laboratories) was diluted in vehicle (5% ethanol, 5% tween 80, 5% PEG40 in water) to a final concentration of 1 mg/ml. This dilution was injected i.p. at 4 mg/kg body weight, five days per week. Control animals were given an equivalent volume of vehicle. Erlotinib (LC Laboratories) was dissolved in 6% Captisol® (Cydex Inc., Lenexa, KS, USA) solution at 5 mg/ml. This solution was then administered at 50 mg/kg body weight by oral gavage, five days per week. Tumor volumes were measured twice weekly by calipers, and tumor volumes were calculated as $\pi/6 * length * width^2$. Mice were dosed with both drugs five days per week, and given two days' rest, for a total of three cycles. At the conclusion of three weeks of treatment, the tumors harvested for histologic and immunohistochemical analysis. Pharmacokinetic samples were drawn with the final dose as follows: at 6 hours post dose, the animals were sacrificed by inhalation overdose of CO₂ and bled by cardiac puncture using EDTA as the anti-coagulant. An aliquot of 50 ul whole blood was frozen at -80C for later analysis of rapamycin. The whole blood was thawed, mixed with 25 ul of 0.2 M Zinc Acetate, and then protein precipitated by the addition of 100 ul of methanol containing 0.15% formic acid, 10 mM NH₄ acetate, and 75 ng/ml of n-benzylbenzamide internal standard. The samples were centrifuged twice at 16,100 × g and the supernatant was analyzed by LC-MS/MS with the following conditions: Buffer A 10 mM Ammonium Acetate in water + 0.1% formic acid; Buffer B 10mM Ammonium Acetate in MeOH + 0.1% formic acid; flow rate 1.5 ml/min; column Agilent C18 XDB column, 5 micron packing 50 X 4.6 mm size ; 0–1 min 100% A, 1–1.5 min gradient to 100% B, 1.5 – 3.0 min 100% B, 3.0–3.1 min gradient to 0% B, 3.1–4.1 100%A; IS N-benzylbenzamide (transition 212.1 to 91.1); Compound transition 931.3 to 864.4. Tumor volumes were compared using two-tailed Student's *t*-test. All animal experiments were performed under protocols approved by the UT Southwestern Institutional Animal Care and Use Committee.

RESULTS

The mTORC1 pathway is active in NSGCTs

We used immunohistochemistry with validated antibodies to probe the status of the mTORC1 signaling in seminomas and in YSTs, a non-seminomatous GCT. YSTs express significantly higher levels of phosphorylation of both mTOR and S6, its downstream target, than do seminomas (Fig. 1A). In agreement with the increased mTORC1 activity, YSTs expressed higher levels of the mTORC1 downstream targets Cyclin D1, HIF1A, and GLUT1 (Fig. 1B). To quantify these results, we assigned each tumor an immunohistochemical staining intensity score ranging from 0 to 9 (Supplementary Table 1). The levels of phospho-mTOR, phospho-S6, CCND1 and HIF1A were all significantly higher in YSTs as compared to seminomas.

To determine whether these immunohistochemistry results were representative of the full clinical spectrum of GCTs, we tested the phosphorylation status of S6 on an independent set of tumors in a series of tumor microarrays representing both seminomas (n=49) and non-seminomas, including YST (n=51, including both Type I and Type II YSTs), choriocarcinomas (n=16) and embryonal carcinomas (n=36). Once again, YST on average showed significantly higher levels of phospho-S6 as compared to seminomas. A substantial

fraction choriocarcinomas and embryonal carcinomas also strongly stained for phosphorylated S6 (Fig. 2A,B and Supplementary Table 2). Overall, Type I YSTs showed slightly higher mean levels of phospho-S6 as compared to Type II YSTs (4.23 ± 3.28 vs. 2.72 ± 2.75); however, this did not reach statistical significance. These results indicate that the mTORC1 pathway is active in a large fraction of NSGCTs.

We next sought to probe the dynamics of mTORC1 signaling and the therapeutic feasibility of mTORC1 inhibition in NSGCT *in vitro*, using two well-characterized embryonal carcinoma cell lines, NTERA-2 and NCCIT. Embryonal carcinoma, the most primitive, undifferentiated NSGCT histology, displayed a wide spectrum of intensity scores in our TMA (Fig. 2B). Using IHC staining of paraffinized cell pellets of each cell line, we confirmed that both cell lines were representative of NSGCTs with high levels of mTORC1 activity (Fig. 2C and Supplementary Table 2).

GCTs express high levels of REDD1, a key negative regulator of mTORC1

We first sought to determine the basis for the lack of mTORC1 activity in seminoma. REDD1 (also known as DDIT4) downregulates mTORC1 activity in response to hypoxic stress in many cell types, including some cancers (33). In spermatogonial stem cells, REDD1 actively inhibits mTORC1 activity to maintain pluripotency (26), and we hypothesized that seminomas could similarly employ REDD1 to suppress mTORC1. Therefore, we stained the tumor samples with REDD1-specific antibodies. It was indeed expressed at significantly higher levels in seminomas than YSTs (Fig. 3 and Supplementary Table 1).

In spermatogonial stem cells, high REDD1 expression is driven by high levels of PLZF. However, PLZF is not higher in seminomas than in YSTs (Fig. 3 and Supplementary Table 1), implying that other factors force high REDD1 expression in seminomas. This result is also consistent with the hypothesis that seminomas as well as nonseminomas arise from a primordial or embryonic germ cell, rather than a spermatogonial stem cell in the adult testis (1). Thus, robust REDD1 expression in seminomas may explain their lack of mTORC1 activation.

EGF and FGF stimulate mTORC1 signaling through MAPK in NSGCTs

We next asked which growth factor pathways might be stimulating mTORC1 activity in NSGCTs. Both seminomas and NSGCTs are known to be driven by *KRAS* or *BRAF* mutation, two genes which drive MAPK signaling (34), and the MAPK and mTORC1 pathways often interact. In some cases, a single cell surface receptor can activate both MAPK and mTORC1 signaling separately (35,36); in other cases the MAPK pathway can directly stimulate mTORC1 activation (36,37). We thus stained our GCT specimens for activated phospho-Erk1/2, one of the key mediators of MAPK signaling. Erk1/2 phosphorylation was seen in both YSTs and seminomas, with a trend toward stronger staining in YSTs though this did not reach statistical significance (Fig. 3 and Supplementary Table 1).

Another possible explanation for differential mTORC1 signaling activity is overexpression of upstream cell surface receptors. To identify cell surface receptors capable of activating

these pathways, we treated GCT cell lines with a panel of extracellular ligands important in NSGCT development (Figure 4 and Supplementary Figure 1). BMP and Wnt ligands, which drive signaling pathways previously shown to be active specifically in NSGCTs (12,14), did not significantly stimulate mTORC1 or MAPK signaling in these cells (Fig. 4A). Interestingly, IGF-II, one of the most well-described activators of phosphoinositide 3-kinase and mTORC1 signaling (38), minimally stimulated mTORC1 and MAPK signaling in the cells (Fig. 4A). One of the risk loci identified in large GCT genome wide association studies is near *SPRY4*, a negative regulator of EGF and FGF2 (23,25). For this reason, we also tested response to EGF and FGF2 in these cells. Strikingly, EGF and FGF2 activated phosphorylation of both ERK1/2 and S6 (Fig. 4A).

To identify the basis for the differential activity of these signaling pathways in seminomas and NSGCTs, we measured the expression of EGF and FGF receptors in YSTs and seminomas. We designed and validated qRT-PCR primers for EGFR and other members of the ErbB family, as well as the four human FGF receptors (Supplementary Table 3). We found that six of the eight ErbB and FGFR family members are expressed at significantly higher levels in YSTs than seminomas (Fig. 4B). These data suggest that NSGCTs activate mTORC1 and MAPK signaling in an EGF- and FGF-dependent manner by expressing higher levels of their receptors.

EGFR and mTORC1 inhibitors synergistically suppress proliferation of GCT cells *in vitro*

Our finding that YSTs frequently exhibit high levels of MAPK and mTORC1 activity suggested that inhibition of these pathways could suppress tumor growth. Consistent with this idea, a recent report by Juliachs and coworkers demonstrated that GCT cells are sensitive to the receptor tyrosine kinase inhibitor lapatinib (39). Cancers are known to escape single-agent mTORC1 inhibition by compensatory upregulation of other pathways, such as through loss of negative feedback on Akt (40). This can be overcome by inhibiting multiple sites in the pathway, such as with a combination of EGFR and mTORC1 inhibitors (41) or with a single-agent dual mTORC1/PI-3 kinase inhibitor (42).

Therefore, we tested the sensitivity of NSGCT cell lines to clinically available pharmacologic inhibitors of EGFR and mTORC1, alone or in combination. Specifically, we exposed NTERA-2 and NCCIT cells to erlotinib and/or rapamycin, small molecule inhibitors of EGFR and mTORC1, respectively (Figure 5 and Supplementary Figures 2 and 3). By treating GCT cells to a range of doses of each drug, we determined the minimum dose required to demonstrate biologic response (Fig. 5A,B). GCT cells exposed to 1 μ M erlotinib or higher demonstrated maximal abrogation of ERK1/2 phosphorylation; similarly, 1 nM rapamycin completely abrogated S6 phosphorylation. These doses are clinically relevant, as they fall below the serum trough concentrations of erlotinib and rapamycin typically achieved in clinical trials (2.9 μ M and 11–16 nM, respectively) (43,44).

These doses were not toxic to NCCIT cells in a 72-hour cell survival assay when given individually (Supplementary Fig. 4). However, to allow time for activation of compensatory pathways, we next exposed these cell lines to erlotinib and/or rapamycin over a longer period of time. Over the course of 7 days, we found that the combination of erlotinib and rapamycin at these clinically achievable doses profoundly reduced cell proliferation (Fig.

5C,D). In NCCIT cells, erlotinib had no effect on proliferation and rapamycin had only a modest effect, but the combination of erlotinib and rapamycin produced a marked cytostatic effect at these doses. NTERA-2 cells, on the other hand, which display stronger basal mTORC1 activity (Fig. 2C), were more sensitive to each inhibitor, and both rapamycin alone and the combination of rapamycin and erlotinib inhibited the growth of the cells.

EGFR and mTORC1 inhibitors synergistically suppress proliferation of GCT cells *in vivo*

Many studies have shown that the antiproliferative effects of drugs on cells in culture can vary widely from effects of the same cells grown *in vivo* as xenografts (45–48). To allow for the possibility that *in vitro* culture conditions affected the sensitivity of GCT cells to the inhibitors, we established xenografts of NCCIT and NTERA-2 cells in immunodeficient mice. When the tumors had reached an average size of ~150 mm³, we initiated treatment with vehicle, erlotinib, rapamycin, or the combination of erlotinib plus rapamycin. We measured the peak plasma concentration of drugs 6 hours after the last dose. For both types of xenografts, combination therapy caused a small increase in the plasma concentration of sirolimus (NT2: 1335+/-176ng/mL alone vs. 1820+/-307 ng/mL combination; NCCIT: 1451+/- 346 ng/mL alone vs. 1834+/-258 ng/mL combination).

We measured tumor sizes over 18 days of therapy. We found that erlotinib monotherapy was not effective against either cell line (Fig. 6). Growth of NTERA-2 xenografts was significantly inhibited by both rapamycin alone and by the combination of erlotinib plus rapamycin (Fig. 6A). In contrast, only the combination therapy was effective against NCCIT xenografts (Fig. 6B). These results largely mirrored what we found with these two cell lines *in vitro*. At the conclusion of treatment, we harvested the xenograft tumors and performed immunohistochemistry for phospho-Erk1/2 and phospho-S6 (Fig. 6C). These tumors were largely necrotic. Erlotinib monotherapy had variable effects and did not completely extinguish ERK phosphorylation, while rapamycin alone clearly extinguished S6 phosphorylation in the xenografts. Combination erlotinib and rapamycin therapy was able to significantly inhibit both ERK and S6 phosphorylation, consistent with the effectiveness of this therapy in impairing the growth of xenografts. Based on these results we conclude that NSGCTs depend on EGFR and mTORC1 signaling for long-term proliferation, and inhibiting these pathways can prevent cell proliferation.

DISCUSSION

There are no viable alternative therapies for the ~15% of GCTs that are resistant to platinum-based therapy (2). Even patients successfully treated face lifelong deleterious effects of chemotherapy (2,49). For these reasons, it is a priority to identify opportunities for targeted therapy of GCTs that might be more effective and less toxic. We focused on NSGCTs as these represent a poorly studied subgroup of GCTs that are more therapy-resistant than seminomas. Here, we identify mTORC1 and EGFR as two novel therapeutic targets in NSGCTs (Supplementary Fig. 5). mTORC1 activity in these tumors appears to be driven by EGF and FGF receptors, and seminomas may suppress mTORC1 activity with high levels of REDD1 in order to maintain an undifferentiated state. Critically, we show that combined small-molecule inhibition of EGFR and mTORC1 blocks the proliferation of

NSGCT cells. Erlotinib was designed to specifically inhibit EGFR-mutant cancers, but it is also clinically active against EGFR-wild-type cancers (50,51). Our results provide the rationale for exploring EGFR and mTORC1 inhibition as adjuvant or alternative therapies for NSGCTs.

In fact, there is data from both preclinical and clinical studies that activation of these pathways may drive cisplatin resistance. Cisplatin-resistant GCT xenografts have increased AKT activation and are amenable to kinase inhibitors including sunitinib and pazopanib (52–54). In addition to these preclinical studies, genetic aberrations of mTORC1 and MAPK pathway genes are especially common in platinum-resistant GCTs (22,55). In addition to previously reported mutations and amplifications of *KIT* and *KRAS*, these groups also found recurrent amplification of *AKT1* and mutations in *FGFR3*, *PIK3CA*, and *MTOR* itself. (Of note, the NCCIT cell line has a known homozygous *PTEN* mutation (Arg173Pro) at a position which is recurrently mutated in other cancers.) To our knowledge, however, no previous studies have actually studied mTORC1 activity in clinical GCT specimens or tested small molecule inhibitors as novel therapeutic strategies.

Our findings also provide significant insight into the biological differences between seminoma and NSGCTs, particularly the differential activation of the mTORC1 pathway despite the prevalence of *AKT1* amplification in both seminomas and nonseminomas. In seminomas, AKT overexpression may drive mTORC1-independent functions, such as loss of apoptosis or cell cycle progression. In fact it has been shown that phosphorylated AKT inhibits apoptosis in a p21-dependent (and, by implication, mTORC1-independent) manner to promote cisplatin resistance in GCT cell lines (56). Thus, in seminomas, overexpression of the mTORC1 negative regulator REDD1 may be required to maintain pluripotency in the face of amplified *AKT*. In NSGCTs, on the other hand, our results suggest that activation of mTORC1 contributes to cell proliferation.

In conclusion, we demonstrate that a significant fraction of malignant NSGCTs display robust activation of EGFR and mTORC1 signaling, and that NSGCT cell lines are sensitive to EGFR and mTORC1 inhibitors. We noted that the peak plasma concentration of rapamycin appeared to be increased by co-administration of erlotinib. We cannot rule out the possibility that this increase account in part for the greater efficacy of combination therapy. However, we do not believe this is the case, as rapamycin alone extinguished S6 phosphorylation in xenografts, and the plasma level achieved by administration of rapamycin alone well already slightly exceeds the level shown to be efficacious in a previous xenograft study (57). Furthermore, combination erlotinib/rapamycin therapy was also more effective in *in vitro* experiments using known concentrations of both drugs. Inhibiting both pathways together may be required to circumvent resistance and provide synergistic cytotoxicity, as has been shown in other cancer models (40,41). Many small molecule inhibitors are in development to target various components of the MAPK and mTORC1 pathways, and future work may identify alternative ways to clinically target these pathways in GCTs. In fact, based on our work, another attractive target may be FGF Receptor.

We also recognize that strategies to inhibit EGF or FGF receptor signaling are likely to be much less effective in tumors with activating *KRAS* or *BRAF* mutations. In these cases,

MEK inhibitors may represent a better strategy, alone or in combination with EGFR/mTORC1 inhibition. As neither of our GCT cell lines harbor activating *KRAS/BRAF* mutations, our study did not address this question. Clinical trials will be required to determine whether such targeted agents are better used alongside traditional platinum-based chemotherapy or whether they should be reserved for salvage regimens in platinum-resistant patients. Such decisions may be guided by *KRAS/BRAF* mutational status. Based on these findings, we believe that EGFR and mTORC1 inhibition represents a promising strategy for targeted therapy in NSGCTs.

Supplementary Material

Refer to Web version on PubMed Central for supplementary material.

Acknowledgments

The authors thank Shama Khokhar (Children's Medical Center Pathology) and Ping Shang and Mohd Alfaraj (UT Southwestern Pathology) for immunohistochemistry, Dr. Jing Liu for assistance with cell survival assays, and the UT Southwestern Preclinical Pharmacology Core Laboratory for assistance with xenografts. REDD1 IHC antibody was a gift of Dr. James Brugarolas.

Financial Support:

Supported by grants from the College of American Pathologists Foundation (DR), the Clinical Development Fund, Department of Pathology, UT Southwestern Medical Center (DR), the Amon G. Carter Foundation (JFA), NIH/National Cancer Institute grants 5R01CA135731 (JFA) and R01CA168761 (LL), The Cancer Prevention and Research Institute of Texas (CPRIT) grants RP110394 (JFA) and RP130212 (LL)RP100119 (LL) and RP110394 (JFA), Welch Foundation grant I-1665 (LL); Welch foundation grant I-1665 (LL); and grant UL1RR024982, titled, "North and Central Texas Clinical and Translational Science Initiative" (Milton Packer, M.D., PI) from the National Center for Research Resources (NCRR), a component of the National Institutes of Health (NIH) and NIH Roadmap for Medical Research. The contents of this manuscript are solely the responsibility of the authors and do not necessarily represent the official view of the NCRR or NIH. Information on NCRR is available at <http://www.ncrr.nih.gov/>. KSC was supported by the Damon Runyon Cancer Research Foundation (DRSG-4P-13) and the W.W. Caruth Research Fellowship from the Children's Medical Center Foundation.

ABBREVIATIONS LIST

EC	embryonal carcinoma
EGF	epidermal growth factor
EGFR	epidermal growth factor receptor
FGF	fibroblast growth factor
FGFR	fibroblast growth factor receptor
GCNIS	germ cell neoplasia in situ
GCT	germ cell tumor
IHC	immunohistochemistry
MAPK	mitogen-activated protein kinase
mTOR	mechanistic target of rapamycin

mTORC1	mTOR complex 1
NSGCT	non-seminomatous GCT
S6	ribosomal protein S6
SEM	seminoma
YST	yolk sac tumor

References

- Oosterhuis JW, Looijenga LH. Testicular germ-cell tumours in a broader perspective. *Nat Rev Cancer*. 2005; 5(3):210–22. [PubMed: 15738984]
- Frazier, AL., Amatruda, JF. Germ Cell Tumors. In: Fisher, DE.Nathan, D., Look, AT., editors. Nathan and Oski's Textbook of Pediatric Hematology-Oncology. London: Elsevier; 2009.
- Amatruda JF, Ross JA, Christensen B, Fustino NJ, Chen KS, Hooten AJ, et al. DNA methylation analysis reveals distinct methylation signatures in pediatric germ cell tumors. *BMC cancer*. 2013; 13(1):313. [PubMed: 23806198]
- Brait M, Maldonado L, Begum S, Loyo M, Wehle D, Tavora FF, et al. DNA methylation profiles delineate epigenetic heterogeneity in seminoma and non-seminoma. *British journal of cancer*. 2012; 106(2):414–23. [PubMed: 22068818]
- Killian JK, Dorssers LC, Trabert B, Gillis AJ, Cook MB, Wang Y, et al. Imprints and DPPA3 are bypassed during pluripotency- and differentiation-coupled methylation reprogramming in testicular germ cell tumors. *Genome Res*. 2016; 26(11):1490–504. [PubMed: 27803193]
- Kraggerud SM, Skotheim RI, Szymanska J, Eknaes M, Fossa SD, Stenwig AE, et al. Genome profiles of familial/bilateral and sporadic testicular germ cell tumors. *Genes, chromosomes & cancer*. 2002; 34(2):168–74. [PubMed: 11979550]
- Coffey J, Linger R, Pugh J, Dudakia D, Sokal M, Easton DF, et al. Somatic KIT mutations occur predominantly in seminoma germ cell tumors and are not predictive of bilateral disease: report of 220 tumors and review of literature. *Genes, chromosomes & cancer*. 2008; 47(1):34–42. [PubMed: 17943970]
- Palmer RD, Barbosa-Morais NL, Gooding EL, Muralidhar B, Thornton CM, Pett MR, et al. Pediatric malignant germ cell tumors show characteristic transcriptome profiles. *Cancer Res*. 2008; 68(11):4239–47. [PubMed: 18519683]
- Oechsle K, Kollmannsberger C, Honecker F, Mayer F, Waller CF, Hartmann JT, et al. Long-term survival after treatment with gemcitabine and oxaliplatin with and without paclitaxel plus secondary surgery in patients with cisplatin-refractory and/or multiply relapsed germ cell tumors. *European urology*. 2011; 60(4):850–5. [PubMed: 21704446]
- Hartmann JT, Nichols CR, Droz JP, Horwich A, Gerl A, Fossa SD, et al. Prognostic variables for response and outcome in patients with extragonadal germ-cell tumors. *Annals of oncology : official journal of the European Society for Medical Oncology / ESMO*. 2002; 13(7):1017–28.
- Shaikh F, Cullen JW, Olson T, Pashankar F, Malogolowkin MH, Amatruda J, et al. Reduced and compressed cisplatin-based chemotherapy in children and adolescents with intermediate-risk extracranial malignant germ cell tumors: A report from the Children's Oncology Group. *J Clin Oncol*. 2016; 34:2016.
- Fustino N, Rakheja D, Ateek CS, Neumann JC, Amatruda JF. Bone morphogenetic protein signalling activity distinguishes histological subsets of paediatric germ cell tumours. *Int J Androl*. 2011; 34(4 Pt 2):e218–33. [PubMed: 21696393]
- Neumann JC, Chandler GL, Damoulis VA, Fustino NJ, Lillard K, Looijenga L, et al. Mutation in the type IB bone morphogenetic protein receptor Alk6b impairs germ-cell differentiation and causes germ-cell tumors in zebrafish. *Proc Natl Acad Sci U S A*. 2011; 108(32):13153–8. [PubMed: 21775673]

14. Fritsch MK, Schneider DT, Schuster AE, Murdoch FE, Perlman EJ. Activation of Wnt/beta-catenin signaling in distinct histologic subtypes of human germ cell tumors. *Pediatr Dev Pathol.* 2006; 9(2):115–31. [PubMed: 16822086]
15. Dmitrovsky E, Murty VV, Moy D, Miller WH Jr, Nanus D, Albino AP, et al. Isochromosome 12p in non-seminoma cell lines: karyologic amplification of c-ki-ras2 without point-mutational activation. *Oncogene.* 1990; 5(4):543–8. [PubMed: 2183156]
16. Looijenga LH, de Leeuw H, van Oorschot M, van Gurp RJ, Stoop H, Gillis AJ, et al. Stem cell factor receptor (c-KIT) codon 816 mutations predict development of bilateral testicular germ-cell tumors. *Cancer Res.* 2003; 63(22):7674–8. [PubMed: 14633689]
17. Rapley EA, Hockley S, Warren W, Johnson L, Huddart R, Crockford G, et al. Somatic mutations of KIT in familial testicular germ cell tumours. *British journal of cancer.* 2004; 90(12):2397–401. [PubMed: 15150569]
18. Fukushima S, Otsuka A, Suzuki T, Yanagisawa T, Mishima K, Mukasa A, et al. Mutually exclusive mutations of KIT and RAS are associated with KIT mRNA expression and chromosomal instability in primary intracranial pure germinomas. *Acta neuropathologica.* 2014; 127(6):911–25. [PubMed: 24452629]
19. Moul JW, Theune SM, Chang EH. Detection of RAS mutations in archival testicular germ cell tumors by polymerase chain reaction and oligonucleotide hybridization. *Genes, chromosomes & cancer.* 1992; 5(2):109–18. [PubMed: 1381946]
20. Olie RA, Looijenga LH, Boerrigter L, Top B, Rodenhuis S, Langeveld A, et al. N- and KRAS mutations in primary testicular germ cell tumors: incidence and possible biological implications. *Genes, chromosomes & cancer.* 1995; 12(2):110–6. [PubMed: 7535083]
21. McIntyre A, Summersgill B, Spendlove HE, Huddart R, Houlston R, Shipley J. Activating mutations and/or expression levels of tyrosine kinase receptors GRB7, RAS, and BRAF in testicular germ cell tumors. *Neoplasia.* 2005; 7(12):1047–52. [PubMed: 16354586]
22. Feldman DR, Iyer G, Van Alstine L, Patil S, Al-Ahmadie HA, Reuter VE, et al. Presence of Somatic Mutations within PIK3CA, AKT, RAS, and FGFR3 but not BRAF in Cisplatin-Resistant Germ Cell Tumors. *Clinical cancer research : an official journal of the American Association for Cancer Research.* 2014
23. Kanetsky PA, Mitra N, Vardhanabhuti S, Li M, Vaughn DJ, Letrero R, et al. Common variation in KITLG and at 5q31.3 predisposes to testicular germ cell cancer. *Nature genetics.* 2009; 41(7):811–5. [PubMed: 19483682]
24. Rapley EA, Turnbull C, Al Olama AA, Dermitzakis ET, Linger R, Huddart RA, et al. A genome-wide association study of testicular germ cell tumor. *Nature genetics.* 2009; 41(7):807–10. [PubMed: 19483681]
25. Poynter JN, Hooten AJ, Frazier AL, Ross JA. Associations between variants in KITLG, SPRY4, BAK1, and DMRT1 and pediatric germ cell tumors. *Genes, chromosomes & cancer.* 2012; 51(3):266–71. [PubMed: 22072546]
26. Hobbs RM, Seandel M, Falciatori I, Rafii S, Pandolfi PP. Plzf regulates germline progenitor self-renewal by opposing mTORC1. *Cell.* 2010; 142(3):468–79. [PubMed: 20691905]
27. Andreassen KE, Kristiansen W, Karlsson R, Aschim EL, Dahl O, Fossa SD, et al. Genetic variation in AKT1, PTEN and the 8q24 locus, and the risk of testicular germ cell tumor. *Human reproduction (Oxford, England).* 2013; 28(7):1995–2002.
28. Caron E, Ghosh S, Matsuoka Y, Ashton-Beaucage D, Therrien M, Lemieux S, et al. A comprehensive map of the mTOR signaling network. *Mol Syst Biol.* 2010; 6:453. [PubMed: 21179025]
29. Hiatt WR, Nissen SE. New drug application 21-628, Certican (everolimus), for the proposed indication of prophylaxis of rejection in heart transplantation: report from the Cardiovascular and Renal Drugs Advisory Committee, US Food and Drug Administration, November 16, 2005, Rockville, Md. *Circulation.* 2006; 113(10):e394–5. [PubMed: 16534016]
30. Kwitkowski VE, Prowell TM, Ibrahim A, Farrell AT, Justice R, Mitchell SS, et al. FDA approval summary: temsirolimus as treatment for advanced renal cell carcinoma. *Oncologist.* 2010; 15(4):428–35. [PubMed: 20332142]

31. Oosterhuis JW, Coebergh JW, van Veen EB. Tumour banks: well-guarded treasures in the interest of patients. *Nat Rev Cancer*. 2003; 3(1):73–7. [PubMed: 12509769]
32. Looijenga LH, Stoop H, de Leeuw HP, de Gouveia Brazao CA, Gillis AJ, van Roozendaal KE, et al. POU5F1 (OCT3/4) identifies cells with pluripotent potential in human germ cell tumors. *Cancer Res*. 2003; 63(9):2244–50. [PubMed: 12727846]
33. Brugarolas J, Lei K, Hurley RL, Manning BD, Reiling JH, Hafen E, et al. Regulation of mTOR function in response to hypoxia by REDD1 and the TSC1/TSC2 tumor suppressor complex. *Genes Dev*. 2004; 18(23):2893–904. [PubMed: 15545625]
34. Sommerer F, Hengge UR, Markwarth A, Vomschloss S, Stolzenburg JU, Wittekind C, et al. Mutations of BRAF and RAS are rare events in germ cell tumours. *International journal of cancer Journal international du cancer*. 2005; 113(2):329–35. [PubMed: 15386408]
35. Choura M, Rebai A. Receptor tyrosine kinases: from biology to pathology. *J Recept Signal Transduct Res*. 2011; 31(6):387–94. [PubMed: 22040163]
36. Lemmon MA, Schlessinger J. Cell signaling by receptor tyrosine kinases. *Cell*. 2010; 141(7):1117–34. [PubMed: 20602996]
37. Langlais P, Yi Z, Mandarino LJ. The identification of raptor as a substrate for p44/42 MAPK. *Endocrinology*. 2011; 152(4):1264–73. [PubMed: 21325048]
38. Pene F, Claessens YE, Muller O, Viguie F, Mayeux P, Dreyfus F, et al. Role of the phosphatidylinositol 3-kinase/Akt and mTOR/P70S6-kinase pathways in the proliferation and apoptosis in multiple myeloma. *Oncogene*. 2002; 21(43):6587–97. [PubMed: 12242656]
39. Juliachs M, Castillo-Avila W, Vidal A, Piulats JM, Garcia Del Muro X, Condom E, et al. ErbBs inhibition by lapatinib blocks tumor growth in an orthotopic model of human testicular germ cell tumor. *International journal of cancer Journal international du cancer*. 2013; 133(1):235–46. [PubMed: 23292912]
40. Wan X, Harkavy B, Shen N, Grohar P, Helman LJ. Rapamycin induces feedback activation of Akt signaling through an IGF-1R-dependent mechanism. *Oncogene*. 2007; 26(13):1932–40. [PubMed: 17001314]
41. Buck E, Eyzaguirre A, Brown E, Petti F, McCormack S, Haley JD, et al. Rapamycin synergizes with the epidermal growth factor receptor inhibitor erlotinib in non-small-cell lung, pancreatic, colon, and breast tumors. *Molecular cancer therapeutics*. 2006; 5(11):2676–84. [PubMed: 17121914]
42. Maira SM, Stauffer F, Brueggen J, Furet P, Schnell C, Fritsch C, et al. Identification and characterization of NVP-BEZ235, a new orally available dual phosphatidylinositol 3-kinase/mammalian target of rapamycin inhibitor with potent in vivo antitumor activity. *Molecular cancer therapeutics*. 2008; 7(7):1851–63. [PubMed: 18606717]
43. Morgenstern DA, Marzouki M, Bartels U, Irwin MS, Sholler GL, Gammon J, et al. Phase I study of vinblastine and sirolimus in pediatric patients with recurrent or refractory solid tumors. *Pediatric blood & cancer*. 2014; 61(1):128–33. [PubMed: 23956145]
44. Hidalgo M, Siu LL, Nemunaitis J, Rizzo J, Hammond LA, Takimoto C, et al. Phase I and pharmacologic study of OSI-774, an epidermal growth factor receptor tyrosine kinase inhibitor, in patients with advanced solid malignancies. *J Clin Oncol*. 2001; 19(13):3267–79. [PubMed: 11432895]
45. Planchon P, Magnien V, Beaupain R, Mainguene C, Ronco G, Villa P, et al. Differential effects of butyrate derivatives on human breast cancer cells grown as organotypic nodules in vitro and as xenografts in vivo. *In Vivo*. 1992; 6(6):605–10. [PubMed: 1296809]
46. Zaugg K, Rocha S, Resch H, Hegyi I, Oehler C, Glanzmann C, et al. Differential p53-dependent mechanism of radiosensitization in vitro and in vivo by the protein kinase C-specific inhibitor PKC412. *Cancer Res*. 2001; 61(2):732–8. [PubMed: 11212276]
47. Lamfers ML, Idema S, Bosscher L, Heukelom S, Moeniralm S, van der Meulen-Muileman IH, et al. Differential effects of combined Ad5- delta 24RGD and radiation therapy in in vitro versus in vivo models of malignant glioma. *Clinical cancer research : an official journal of the American Association for Cancer Research*. 2007; 13(24):7451–8. [PubMed: 18094429]
48. Triozzi PL, Aldrich W, Dombos C. Differential effects of imatinib mesylate against uveal melanoma in vitro and in vivo. *Melanoma Res*. 2008; 18(6):420–30. [PubMed: 18971787]

49. Hale GA, Marina NM, Jones-Wallace D, Greenwald CA, Jenkins JJ, Rao BN, et al. Late effects of treatment for germ cell tumors during childhood and adolescence. *J Pediatr Hematol Oncol.* 1999; 21(2):115–22. [PubMed: 10206457]
50. Osarogiagbon RU, Cappuzzo F, Ciuleanu T, Leon L, Klughammer B. Erlotinib therapy after initial platinum doublet therapy in patients with EGFR wild type non-small cell lung cancer: results of a combined patient-level analysis of the NCIC CTG BR.21 and SATURN trials. *Transl Lung Cancer Res.* 2015; 4(4):465–74. [PubMed: 26380188]
51. Neumair P, Joos L, Warschkow R, Dutly A, Ess S, Hitz F, et al. Erlotinib has comparable clinical efficacy to chemotherapy in pretreated patients with advanced non-small cell lung cancer (NSCLC): A propensity-adjusted, outcomes research-based study. *Lung Cancer.* 2016; 100:38–44. [PubMed: 27597279]
52. Castillo-Avila W, Piulats JM, Garcia Del Muro X, Vidal A, Condom E, Casanovas O, et al. Sunitinib inhibits tumor growth and synergizes with cisplatin in orthotopic models of cisplatin-sensitive and cisplatin-resistant human testicular germ cell tumors. *Clinical cancer research : an official journal of the American Association for Cancer Research.* 2009; 15(10):3384–95. [PubMed: 19417025]
53. Juliachs M, Vidal A, Del Muro XG, Piulats JM, Condom E, Casanovas O, et al. Effectivity of pazopanib treatment in orthotopic models of human testicular germ cell tumors. *BMC cancer.* 2013; 13:382. [PubMed: 23937707]
54. Juliachs M, Munoz C, Moutinho CA, Vidal A, Condom E, Esteller M, et al. The PDGFRbeta-AKT pathway contributes to CDDP-acquired resistance in testicular germ cell tumors. *Clinical cancer research : an official journal of the American Association for Cancer Research.* 2014; 20(3):658–67. [PubMed: 24277456]
55. Wang L, Yamaguchi S, Burstein MD, Terashima K, Chang K, Ng HK, et al. Novel somatic and germline mutations in intracranial germ cell tumours. *Nature.* 2014; 511(7508):241–5. [PubMed: 24896186]
56. Koster R, di Pietro A, Timmer-Bosscha H, Gibcus JH, van den Berg A, Suurmeijer AJ, et al. Cytoplasmic p21 expression levels determine cisplatin resistance in human testicular cancer. *The Journal of clinical investigation.* 2010; 120(10):3594–605. [PubMed: 20811155]
57. Sivanand S, Pena-Llopis S, Zhao H, Kucejova B, Spence P, Pavia-Jimenez A, et al. A validated tumorgraft model reveals activity of dovitinib against renal cell carcinoma. *Sci Transl Med.* 2012; 4(137):137ra75.

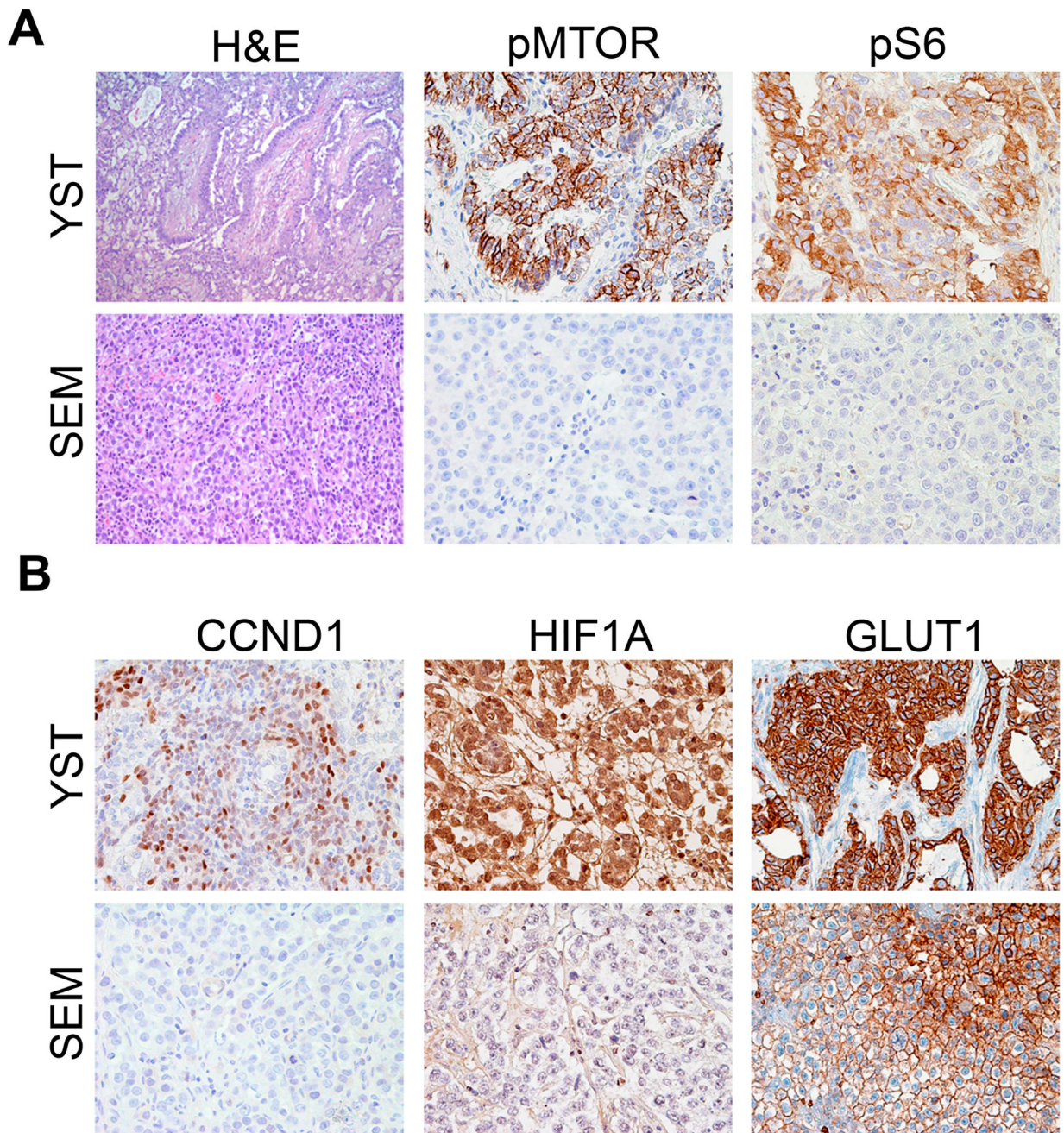


Figure 1. mTORC1 signaling is active in yolk sac tumors

Immunohistochemical staining of seminoma (SEM) and yolk sac tumor (YST) samples for mTORC1 signaling components. A, staining for the phosphorylated forms of mTOR and S6. B, staining for mTORC1 target genes CCND1, HIF1A, and GLUT1.

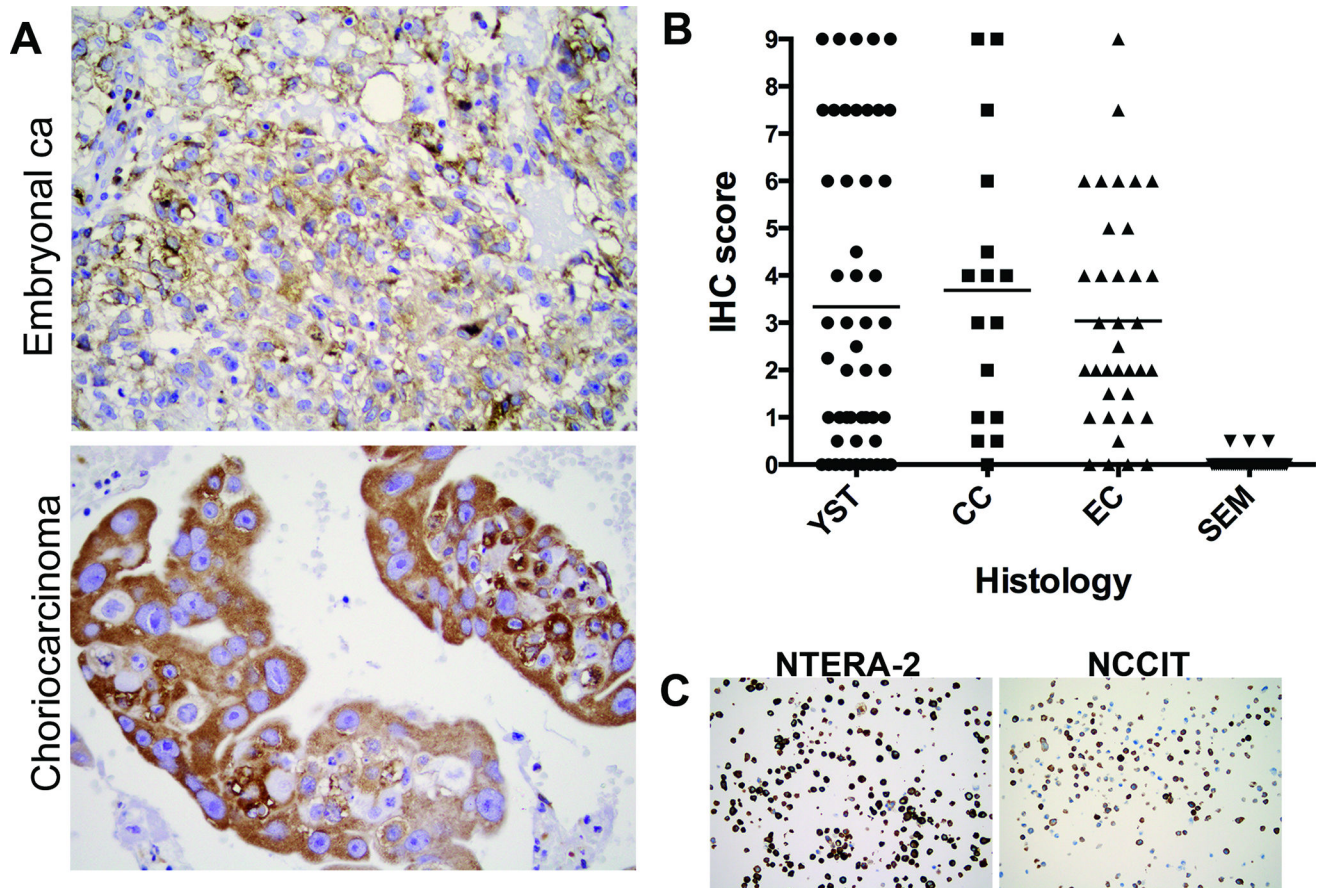


Figure 2. Other nonseminomatous GCT histologies also exhibit highly active mTORC1 signaling
 A, IHC staining for phosphorylated S6 in embryonal carcinoma (top) and choriocarcinoma (bottom). B, phospho-S6 IHC intensity score in GCT histologies. Horizontal bar represents mean values for each histology. YST: yolk sac tumor; CC: Choriocarcinoma; EC: Embryonal Carcinoma; SEM: Seminoma. *p*-values for comparison with SEM: YST <0.001; CC 0.0002; EC <0.0001 (2-tailed Student's *t*-test). C, IHC for phosphorylated S6 in NCCIT and NTERA-2 cells.

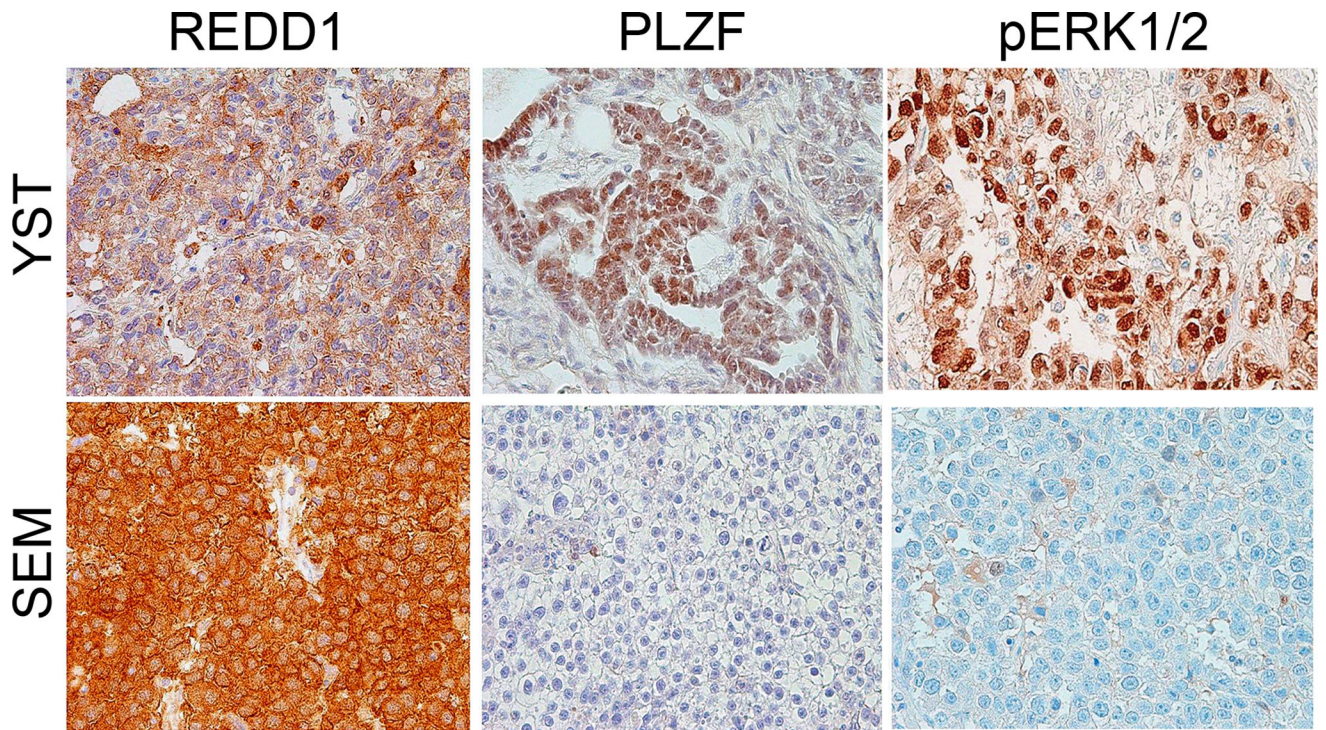


Figure 3. Immunohistochemical staining of other markers in germ cell tumors
Immunohistochemical staining of yolk sac tumor (YST) and seminoma (SEM) samples for REDD1, PLZF, and the phosphorylated form of ERK (T202/204).

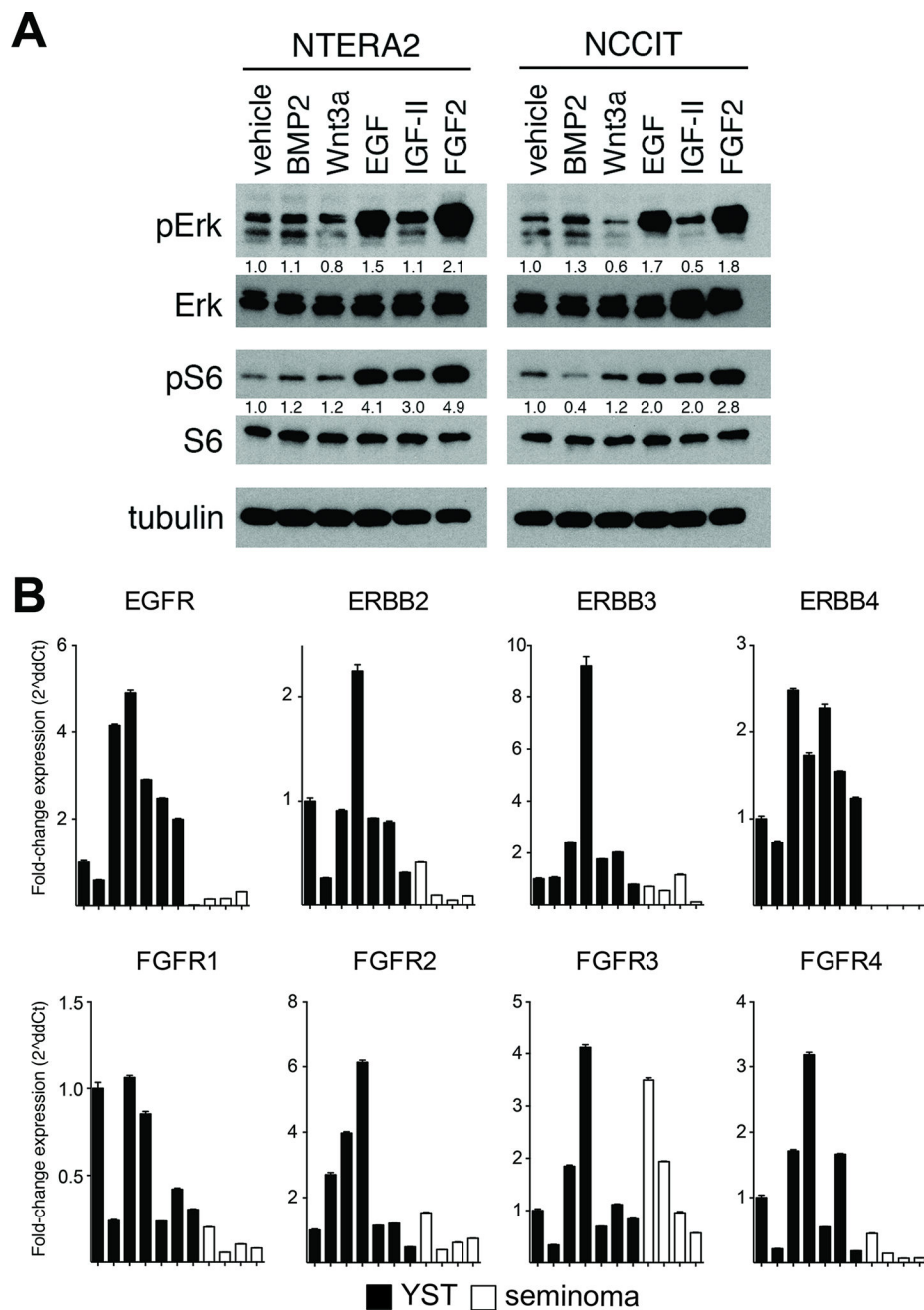


Figure 4. EGF and FGF2 ligands stimulate mTORC1 and MAPK signaling in GCT cells
 A, Immunoblots for phospho-Erk1/2 and phospho-S6 in lysates harvested from NCCIT cells after exposure to ligand for 20 minutes. Relative ratio of intensity of phosphorylated to total protein calculated by densitometry. See Supplementary Figure 1 for complete blots. B, Quantitative RT-PCR of tumor RNA showing relative expression of ErbB and FGFR family members in seven YST and four seminoma samples. Values represent mean \pm SD; * $p < 0.05$.

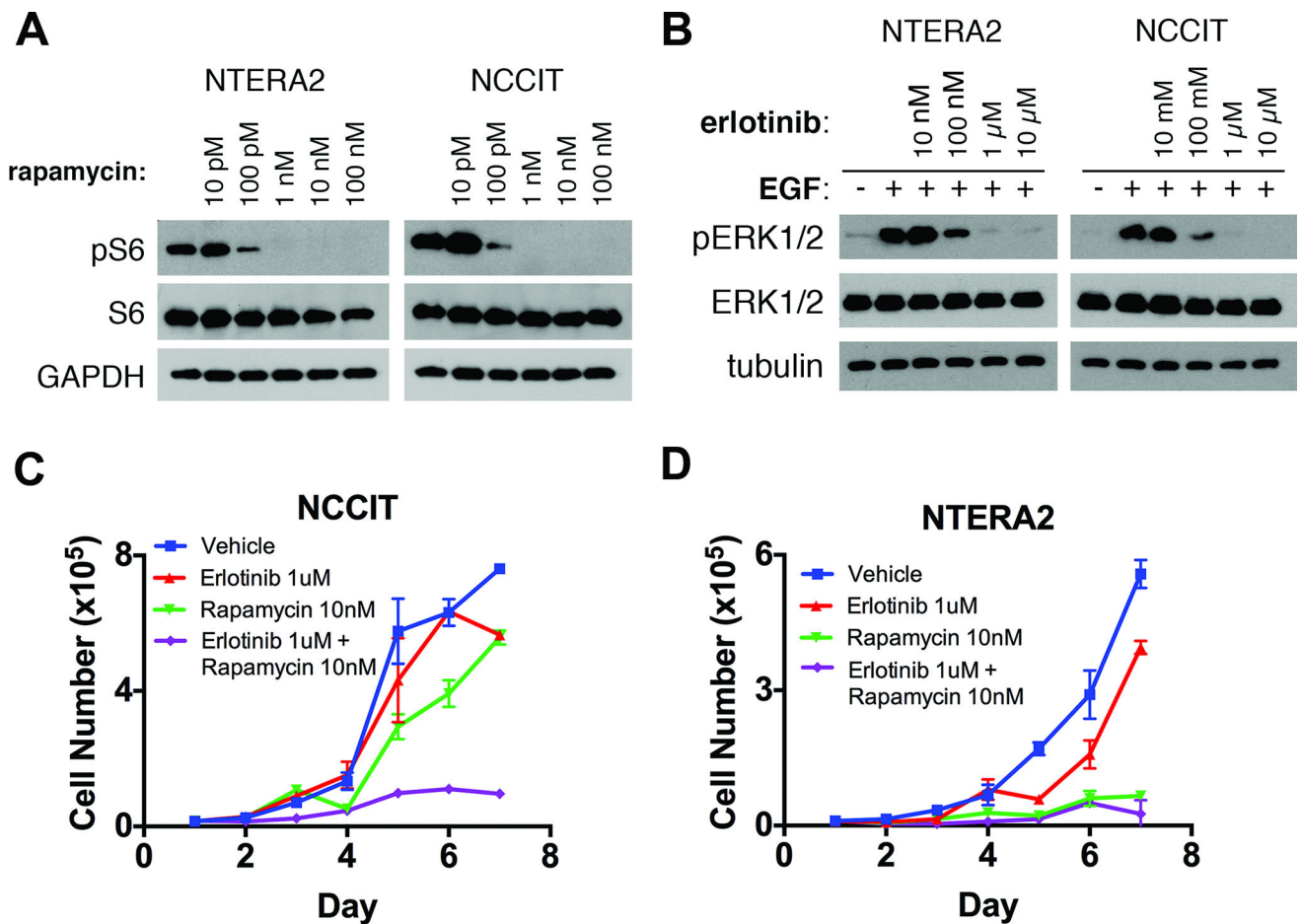


Figure 5. EGFR and mTOR inhibitors decrease proliferation of GCT cells in vitro

A, Immunoblots showing response of mTOR phosphorylation to a range of rapamycin doses in NCCIT and NTERA2 cells exposed to drug for 12 hours in serum-starved conditions. See Supplementary Figures 2 and 3 for complete blots. B, Immunoblots showing response of Erk1/2 phosphorylation to a range of erlotinib doses in NCCIT cells exposed to drug for 12 hours in serum-starved conditions. C, D, Cell proliferation of (C) NCCIT and (D) NTERA-2 cells in the presence of erlotinib, rapamycin, or the combination.

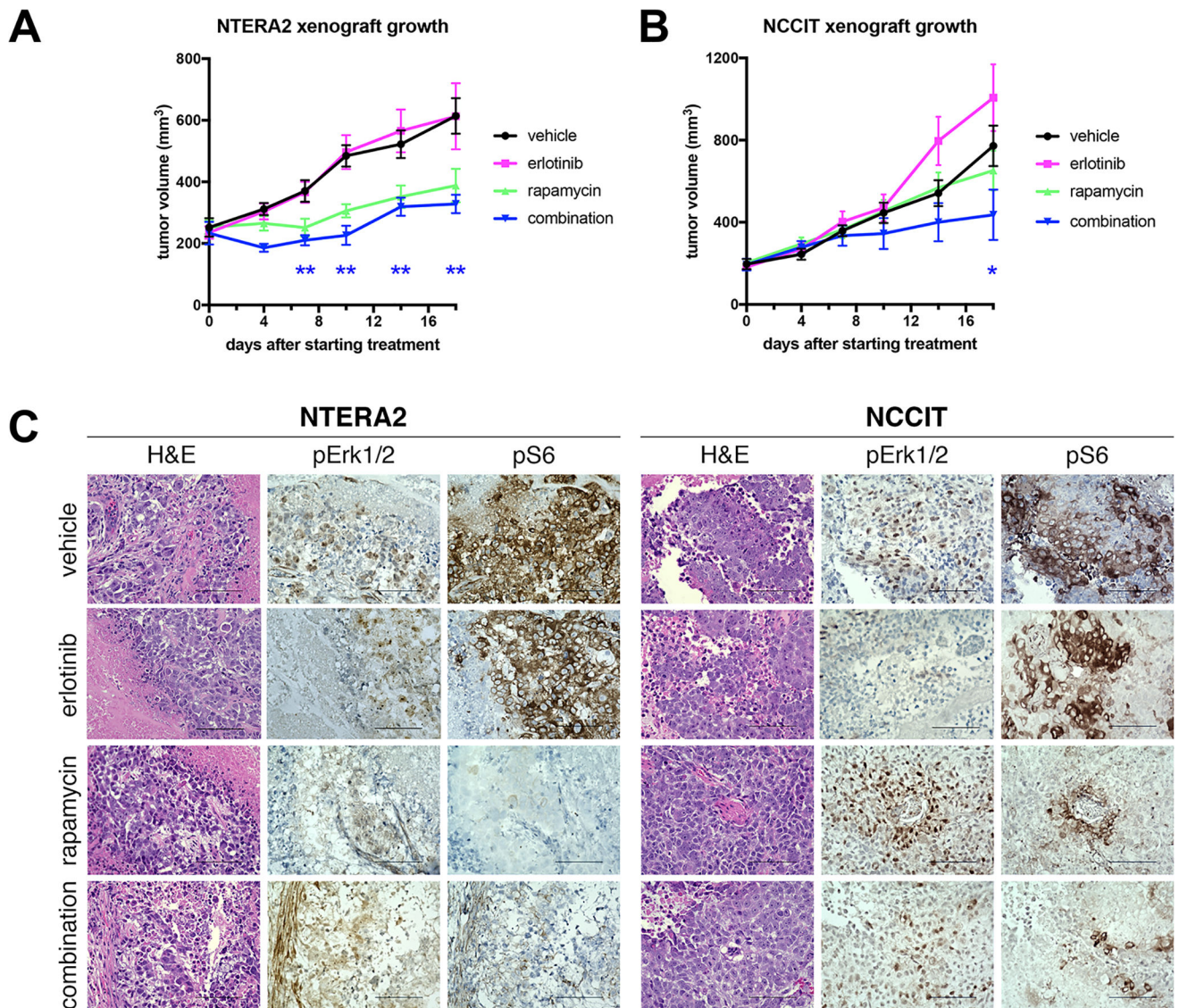


Figure 6. Combined EGFR and mTOR inhibition impairs germ cell tumor growth in vivo
 A, B, Effect of EGFR and mTOR inhibitors on growth of xenografts of NTERA-2 (A) and NCCIT (B) in immunocompromised mice, expressed in tumor volume. * $p < 0.05$, ** $p < 0.01$ by two-tailed t -test between combination vs. vehicle control. $N=8$ mice in each group, except for $n=7$ in NCCIT combination group, because one mouse died from an inadvertent overdose. C, representative immunohistochemistry images of xenograft tumors from mice treated with the indicated inhibitors and stained with antibody specific for the phosphorylated ERK (pERK) or phosphorylated ribosomal protein S6 (pS6).